Effects of Target Fragmentation on Evaluation of LET Spectra From Space Radiation in Low-Earth Orbit (LEO) Environment: Impact on SEU Predictions

J. L. Shinn, F. A. Cucinotta, and J. W. Wilson
NASA Langley Research Center
Hampton, VA 23681-0001

G. D. Badhwar and P. M. O'Neill
NASA Johnson Space Center
Houston, TX 77058

F. F. Badavi
Christopher Newport University
Newport News, VA 23606-2998

Abstract

Recent improvements in the radiation transport code HZETRN/BRYNTRN and galactic cosmic ray environmental model have provided an opportunity to investigate the effects of target fragmentation on estimates of single event upset (SEU) rates for spacecraft memory devices. Since target fragments are mostly of very low energy, an SEU prediction model has been derived in terms of particle energy rather than linear energy transfer (LET) to account for nonlinear relationship between range and energy. Predictions are made for SEU rates observed on two Shuttle flights, each at low and high inclination orbit. Corrections due to track structure effects are made for both high energy ions with track structure larger than device sensitive volume and for low energy ions with dense track where charge recombination is important. Results indicate contributions from target fragments are relatively important at large shield depths (or any thick structure material) and at low inclination orbit. Consequently, a more consistent set of predictions for upset rates observed in these two flights is reached when compared to an earlier analysis with CREME model. It is also observed that the errors produced by assuming linear relationship in range and energy in the earlier analysis have fortuitously canceled out the errors for not considering target fragmentation and track structure effects.

I. INTRODUCTION

The demands for reducing the size and power requirements of future spacecraft leads to designs which efficiently process large quantities of data onboard to reduce the amount of telemetry. Such an approach leads to designs utilizing high density digital devices which are more susceptible to single event upsets (SEU). Accurate prediction of SEU rates for spacecraft computers in orbital environments is needed for cost-effective system designs. The accuracy is determined by several factors, such as device interaction models, accelerator measurements and interpretation of measured data, environmental models external to the spacecraft, and transport calculations for modified environments internal to the shield. Although progress has occurred in these areas, as described and summarized by Petersen et al. [1], uncertainties in existing external and internal environmental models are still very large. Recently, improvements have been made by Badhwar and O'Neill in predicting the free-space galactic cosmic ray (GCR) energy spectrum [2]. Their model was tested against the LET spectra measured on several Space Shuttle flights [3]. A detailed comparison of the measurement with tissue equivalent proportional counters (TEPC) with predictions obtained using the model [2] and the radiation transport code HZETRN/BRYNTRN [4–7] shows overall agreement to within ±15 percent for the absorbed and equivalent dose but with some discrepancy in LET spectra. The underprediction at lower LET suggested the need for including the secondary pion and kaon fluxes in the code and developing an improved understanding of the detector response due to delta rays and wall effect [3]. The underprediction in the higher LET region requires further refinement of the energy spectra of target and knock-on particles. Recently, modifications have been made in the code to include explicit description of the energy spectra of heavy ion target fragments and refinements in those of the light ion secondaries [7,8] thus improving the calculation for high LET spectra, critical to SEU evaluations.

Target fragments are mostly produced by energetic protons, neutrons, and some light ions in the LEO environment. In the primary GCR, ^{4}He is the most abundant nucleus after ^{1}H. Since the GCR spectrum is broad with a peak at several hundred MeV/A with an appreciable number of particles out to about 10–50 GeV/A, fragmentation of the multiple charged ions is dominant in GCR transport. The light mass particles have longer ranges and great multiplicity in

elastic nuclear events, leading to a buildup in their number in shielding. Estimation of upset rates due to these particles becomes important when GCR and trapped protons pass through a bulk material. Rather than relying on costly laboratory SEU cross section measurements for these particles, several investigators [9–11] have attempted in the past to predict proton or neutron SEU rate from low energy heavy-ion test data. The methods used to obtain nuclear reaction products were mostly time-consuming Monte Carlo simulations, unlike HZETRN/BRYNTRN code which calculates nuclear reaction products very efficiently.

O'Neill and Badhwar recently made a preliminary analysis for the measured SEU rate of SRAM memories situated at the Space Shuttle general -purpose computers (GPC's) for several shuttle flights [12]. The transport calculations [12] were made using the CREME (Cosmic Ray Effects on Microelectronics) code [13], with the model from reference [2] serving as the input GCR spectrum. The results indicate a need for a more exact transport calculation which would account for the target fragments from the breakup of shield nuclei, particularly for low inclination orbits. It is anticipated that inclusion of target fragmentation will reduce the inconsistency in their comparison between low and high inclination orbits. In this work, we will revisit the problem for incident GCR by developing a SEU prediction model suitable for low energy target fragments and describing the necessary corrections for track structure effects on the available charge for upset. The transport calculation has been made using the newly modified HZETRN/BRYNTRN code which calculates very efficiently both projectile and target fragment energy spectra for 59 isotopes from neutrons up to iron ions.

II. GALACTIC ION TRANSPORT MODEL

The propagation of the GCR and their secondaries through bulk matter is described by the Boltzmann equation which in the straight ahead approximation is of the form [5,14]

$$\left[\frac{\partial}{\partial x} - \nu_j \frac{\partial}{\partial E} S(E) + \sigma_j(E)\right]\phi_j(E) = \sum_k \int_0^\infty f_{jk}(E,E')\phi_k(x,E')\,dE' \tag{1}$$

where ν_j denotes the range scaling parameter which is equal to Z_j^2 / A_j; where A_j and Z_j are the mass and charge numbers of ion j, respectively. In equation (1), E represents energy (MeV/A), $S(E)$ is the proton stopping power, $\sigma_j(E)$ is the total cross section, $\phi_j(x,E)$ is the differential flux spectrum, and $f_{jk}(E, E')$ is the differential energy cross section for redistribution of particle type and energy through elastic scattering or nuclear reaction such as fragmentation. The numerical solution to equation (1) has been developed by Wilson et al. [14] using the method of characteristics with the production terms separated into projectile fragmentation and target fragmentation terms.

The HZETRN code (for which BRYNTRN is a subset for the light particle transport) uses energy dependent nuclear interaction cross sections and assumes realistic energy spectra for low mass particles (A < 4) [7,15]. Inclusion of the energy dependent nuclear cross sections was shown to have a large effect on the highest LET components [16] and is essential to predicting SEU rates from GCR. For heavy ion projectile fragmentation, secondaries are assumed to be produced at the velocity of the primaries. Further details on the transport methods and data base are found in [5,15,16].

The input free-space GCR spectrum is calculated using the model of Badhwar and O'Neill [2]. The value of the deceleration potential required as input to this model was derived from the measured Climax neutron monitor count rate which varies over the 22-year solar cycle. The standard GCR model commonly used to predict SEU rates is the Cosmic Ray Effects on Microelectronics (CREME) code [13] which accounts only for 11-year solar cycle modulation (represented by a simple sine variation) and does not distinguish between odd-even cycles with 22 year period. For low earth orbit, the geomagnetic cutoff given by Shea and Smart [17] later coded by Adams et al. [18] is used. The HZETRN and the model of Badhwar et al. have been tested with several Shuttle flight experiments using passive detectors (TLD and nuclear track detectors) as well as active detectors (tissue equivalent proportional counters and a charged particle spectrometer telescope) and appeared to be in reasonable agreement between model predictions and measurement overall [8] but some differences remain unresolved as described in Section 1.

We further compare the results of the HZETRN code using environmental model of Badhwar and O'Neill with the measurements of Wiegel et al. [19] using CR39 track detectors. Their measurements include both the contributions of the HZE particles (primaries and their fragments) and the low energy target fragments. The short range target fragments were identified as adjacent etch cones across the interface of two track foils and no entrance track at the top of the stack. The etching process removes 40 μm at the foil interface so that only those tracks of 40 μm and greater length are counted. In addition, many of the isotropically produced target fragments not counted must have greater range if they are oblique to the interface. We account for the etching loss of short range tracks resulting in reduced contributions from low energy fragments. Figure 1 shows the comparison of measured LET spectra for D1 mission (first German Spacelab mission) obtained by Wiegel et al. [19] with the current environmental and transport model. There is a vast improvement of HZETRN with its current environmental model to predict the CR39 result over the results given in Figure 1 of reference 19. Unlike earlier calculational models

[19], the trends in the measurement are well represented by the calculations at a single depth of 20–30 g/cm^2. Not least of these improvements is the fragmentation model improvements in the lower LET region.

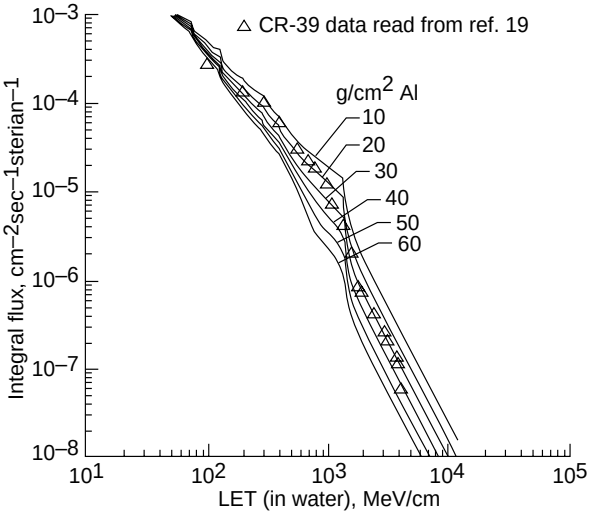

Fig. 1 Comparison of measured LET spectra for D1 mission with HZETRN calculation with solid lines representing spectra behind various thicknesses of Al.

III. Single Event Upset Model

Direct Ionization

The device upset results from the release of energy by ions to generate electron-hole pairs resulting in a current of sufficient magnitude to switch state in the device. It is usually assumed that the single parameter critical charge is independent as to where the free charges are formed within the sensitive volume; whereas in reality there is a charge collection efficiency and charge recombination effect (for a dense track) depending on the initial charge distribution. The charge generated is related to the energy deposit as

$$Q \text{ (in pC)} = \varepsilon \text{ (in MeV)} /22.5 \tag{2}$$

It is customary to assume that an upset occurs if $Q \geq Q_C$ corresponding to a critical energy $\varepsilon_C = 22.5\, Q_C$. In this case, the upset event for a given particle traversal is reduced to estimating the energy loss in crossing the sensitive volume.

In a uniform isotropic radiation environment as often found in a spacecraft, the number of particles entering the device sensitive volume is

$$dN_i = \pi A\, \phi_i(E)\, dE \tag{3}$$

where $\phi_i(E)\, dE$ is the omnidirectional fluence of particles of type i between energies E and $E + dE$ and A is the total surface area of the sensitive volume. The particles arrive randomly along various rays with a distribution of chords of length s given as $f(s)$. The number of particles with chord length between s and $s + ds$ is

$$dN_i = \pi A\, f(s)\, ds\, \phi_i(E)\, dE \tag{4}$$

The energy loss by the particle along the chord is

$$\varepsilon = E - R_i^{-1}\left[R_i(E) - s\right] \tag{5}$$

where $R_i(E)$ is range of particle i of energy E, and $R_i^{-1}(x)$ is the residual energy for a particle i of residual range x. (Note, R and R^{-1} are operators such that $R_i^{-1}\left[R_i(E)\right] = E$). Associated with the critical energy is a critical chord s_C given by

$$\varepsilon_C = E - R_i^{-1}\left[R_i(E) - s_C\right] \tag{6}$$

which may be solved as (for $E \geq \varepsilon_C$)

$$s_C = R_i(E) - R_i(E\text{-}\varepsilon_C) \tag{7}$$

At the lower energy end of a typical GCR spectrum, all particles of energy E will cause an upset when traversing the sensitive volume along chords of length greater than s_C. At the high energy end, only those particles depositing energy greater than ε_C after traversing a distance limited by the longest chord $s_{\max}$ of the sensitive volume will cause an upset. The total number of upsets is

$$dN = \int_{s_C}^{s_{\max}} f(s) ds\, \pi A \phi_i(E)\, dE \tag{8}$$

Note that s_C depends on both particle type and energy. The total upsets caused by all particles and energies is

$$N = \sum_i \int_0^{\infty} \int_{s_C}^{s_{\max}} f(s)\, ds\, \pi A \phi_i(E)\, dE \tag{9}$$

which may be calculated as

$$N = \sum_i \int_0^{\infty} F(s_C)\, \pi A \phi_i(E)\, dE \tag{10}$$

where $F(s_C)$ is the integral pathlength (chord) distribution.

Another form of equation (10) can be obtained by first approximating the critical chord by a Taylor series as

$$s_C \cong \varepsilon_C / L(E) + O(\varepsilon_C^2) \tag{11}$$

where L is the linear energy transfer (LET). Retention of the first term is equivalent to assuming L being constant along the chord. One may rewrite N as

$$N = \sum_i \int_0^{\infty} \int_{\varepsilon_c / L}^{s_{\max}} f(s)\, ds\, \pi A \phi_i(L)\, dL$$

$$= \pi A \sum_i \int_0^{s_{\max}} f(s) \int_{\varepsilon_c / s}^{\infty} \phi_i(L)\, dL\, ds \qquad (12)$$

$$= \pi A \sum_i \int_0^{s_{\max}} f(s)\, \Phi_i(\varepsilon_c / s)\, ds$$

where $\Phi_i(L)$ is the integral LET spectrum. A change of variables as $L = \varepsilon_c/s$ results in

$$N = \sum_i \pi A\, \varepsilon_i \int_0^{\infty} f(\varepsilon_c / L)\, \Phi_i(L)\, dL / L^2 \qquad (13)$$

consistent with the results used in the CREME code. The CREME results require validity of the Taylor series expansion which is only satisfied at high energies for $R_i(E) >> s_c$.

Since most test data do not produce a sharp step function for the SEU cross section measurement, it is customary to understand this behavior in terms of distributed device elements with varying upset sensitivity. We follow the usual custom and perform an expected value calculation [20] for the upset rate $\overline{N}$ by integrally weighting $N(\varepsilon_c)$ with the normalized experimental cross section curve

$$\overline{N} = \int_{\varepsilon_{\min}}^{\infty} N(\varepsilon_c)\, g(\varepsilon_c)\, d\varepsilon_c \qquad (14)$$

where $\varepsilon_{\min}$ is the minimum threshold energy and $g(\varepsilon_c)$ is the probability density distribution function related to the cumulative distribution function as represented by the normalized experimental cross section curve. We further approximate the integral over ε_c with summation by dividing the measured cross section curve into several steps thus yielding small surface areas. Substituting equation (13) into equation (14) one obtains

$$\overline{N} = \pi \sum_j A_j \sum_i \int_{\varepsilon_{cj}}^{E_{\max}} F(s_c)\, \phi_i(E)\, dE \qquad (15)$$

where A_j is the total surface area of step j and $\varepsilon_{cj} = L_{th\,j} \bullet t$ with t being the charge collection length and $L_{th\,j}$ corresponds to the LET threshold for the j-th step. Note that if one uses equation (10) rather than equation (13) for equation (14), one obtains an SEU rate expression similar to equation (2) in reference [12] except that the charge collection length t does not change with the choice of steps but rather is given by the real physical size. Since equation (10) is more accurate than equation (13) in evaluating the low energy target fragments, equation (15) is used in this work.

Track Structure Effect

The response of materials to passing ions is related to the amount of local energy deposited and the manner in which that energy is deposited. The scale of delta-ray track emanating from the core of particle track varies widely according to the energy and charge of passing ions as seen in nuclear emulsion. At very large energy per unit mass, the track width is usually many microns causing energy deposit beyond the sensitive site (carried by secondary electrons). In this work, the fraction of energy deposited within the sensitive volume over the energy loss as given by Xapsos [21] will be used to correct for large particle track width. For low energy high-LET target fragments, the charges created along the core are so dense that charge recombination reduces the amount of available charge for upset. A simple charge generation and recombination model developed for the high-LET fragments is described below.

The energy release by the passing ions is through collisional excitation of orbital electrons of atoms within the device to high momentum states. These electrons in turn diffuse from the collision site transferring significant amounts of the kinetic energy received from the ion to other electrons as the initial energy released is degraded and distributed about the ion path. The electron slowing down spectra are remarkably independent of the initiating event as the collisional transfer among electrons dominates the diffusion process. Ultimately, the energy resides in subexcitation electrons which thermalize and recombine with the holes produced in the media or are passed through the external circuit of the device. Recombination is dominated by Auger transitions and follow the kinetic equations

$$\frac{dn}{dt} = -kn^2 \qquad (16)$$

where we assume the electrons and hole densities are similarly distributed. The time development of the electron density is

$$n(t) = \frac{n_0}{1 + n_0 k\tau} \qquad (17)$$

We follow Martin et al. [22] and consider the degree of recombination in the device charge recombination time τ before charge collection occurs where $(k\tau)^{-1} \approx 5\text{x}10^{20}$ /cm^3 for 10 ps. The initial density can be found from the work of Cucinotta et al. [23] as

$$n_0(r) = D(r)/W \qquad (18)$$

where

$$D(r) = \frac{2.33 \times 0.085 Z^2}{4\pi\beta^2} \quad \frac{10^7 r}{1 + (0.6 + 1.8\beta)10^7 r} \times \frac{1}{r^2} \exp\left[-(r / 0.37\, r_{\max})^2\right] \qquad (19)$$

is the absorbed energy per unit volume, $r_{\max}$ is the maximum electron range resulting from the ion collision, and

W is 3.6 eV per ion pair formed. Thus, the collectable charge distribution (after recombination) is approximately

$$n(\tau, r) = \frac{n_0(r)}{1 + n_0(r) k\tau} \tag{20}$$

from which the total charge produced by the ion passage can be calculated. The initial charge produced per unit pathlength of the ion is

$$Q_0 = \int_0^\infty 2\pi\, r\, n_0(r)\, dr \tag{21}$$

The fractional charge remaining after recombination for several ions is given by

$$\frac{Q(\tau)}{Q_0} = \int_0^\infty 2\pi r\, n(\tau, r)\, dr \Big/ \int_0^\infty 2\pi r\, n_0(r)\, dr \tag{22}$$

Figure 2 shows the results for a charge recombination time of 50 ps which is arbitrarily taken for illustrative purpose.

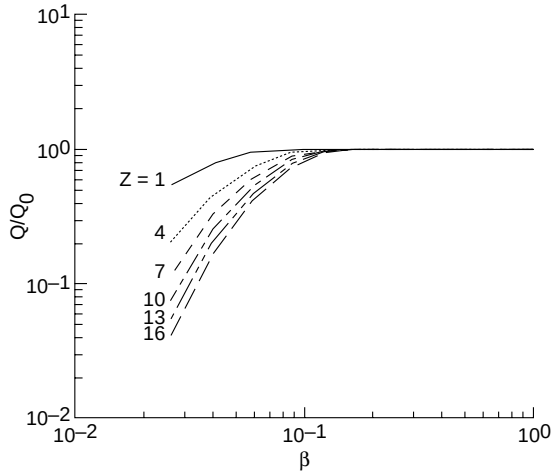

Fig. 2 Fractional charge remaining in ion track core as function of β (ion velocity divided by speed of light) for various ions of charge *Z* after 50 ps of Auger recombination.

IV. Shuttle Data Analyses

The Space Shuttle general purpose computers were upgraded with IMS1601EPI SRAM to replace original magnetic core memories in 1991. The contributions to SEU rates recorded in many shuttle flights were previously analyzed and separated [12] into two sources: GCR and South Atlantic Anomaly. In this study, only the contribution from GCR on two shuttle flights are considered: STS-56 in 57.1 degree inclination orbit and STS-51 in 28.5 degree. The input GCR spectra with geomagnetic cutoff are propagated through 100 g/cm^2 of aluminum shield using HZETRN/BRYNTRN code. Shuttle orbiter shielding is accounted for by obtaining energy spectra at eleven different thicknesses (3, 5, 8, 12, 20, 30, 40, 55, 70, 85, and 100 g/cm^2) that cover the range of thickness for the computer location in the orbiter. The aluminum equivalent thickness of the orbiter body was determined for 968 rays uniformly distributed in all directions emanating from the computer location. The fraction for the number of rays (or fraction of solid angle) at these eleven thicknesses are given in Table 1. The energy spectra resulting from the transport calculation at each of the eleven depths are then used in Equation (15) to obtain SEU rates which in turn are weighted with the distribution given in Table 1 to give the combined SEU rate predicted for the orbiter.

Table 1. Shuttle Shield Distribution

Equivalent aluminum thickness, g/cm^2	Fraction of solid angle
3	.100
5	.142
8	.086
12	.054
20	.082
30	.109
40	.113
55	.170
70	.055
85	.045
100	.044

The experimental SEU cross section curve for IMS1601EPI used in previous analyses [12] is shown in Figure 3 and is used in equation (15) to predict error rates. Here we still assume the geometry of sensitive volumes to be rectangular parallelpiped with an assumed thickness to width ratio of about 0.1, yet at each step for carrying out the summation in equation (15) the critical energy is related to the LET threshold at each step with an thickness of about 1 μm. The degree of charge recombination assumed here is $(k\tau)^{-1} = 5\text{x}10^{20}/\text{cm}^3$.

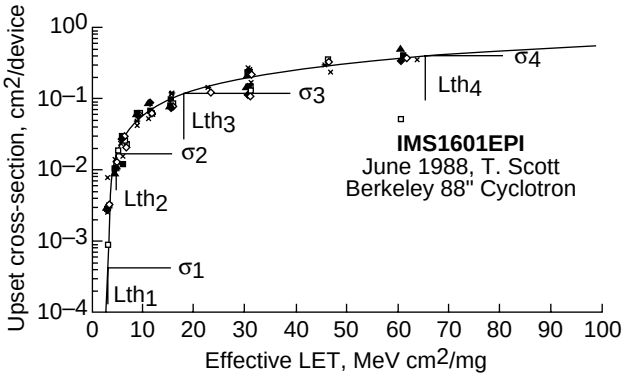

Fig. 3 Measured heavy ion single event upset integral cross section versus effective LET for IMS1601EPI as given in reference 12.

V. Results and Discussion

A calculated LET spectra for projectiles and their fragments, excluding target fragments other than nucleons, is shown in Figure 4 for GCR integral fluxes propagated through aluminum shield thicknesses of 55 g/cm^2 at STS-56 flight conditions. Also shown are the spectra with light ion fragments ($Z < 3$) added, and with all the fragments (all Z) added. The increase due to heavier target fragments is above 1050 MeV/g/cm^2 while increase caused by light ions is slightly below that. The lowest threshold for SEU seen in Figure 3 is 2.5 MeV/mg/cm^2 (2500 MeV/g/cm^2). With the sensitive volume thickness to width ratio of 0.1, an increase in the integral flux above 250 MeV/g/cm^2 will affect the calculated SEU rate. Although the increase in flux due to added target fragment contributions is about one to two orders of magnitude larger than without in the LET region of interest, their contributions are greatly reduced by the track structure effect shown in Figure 2.

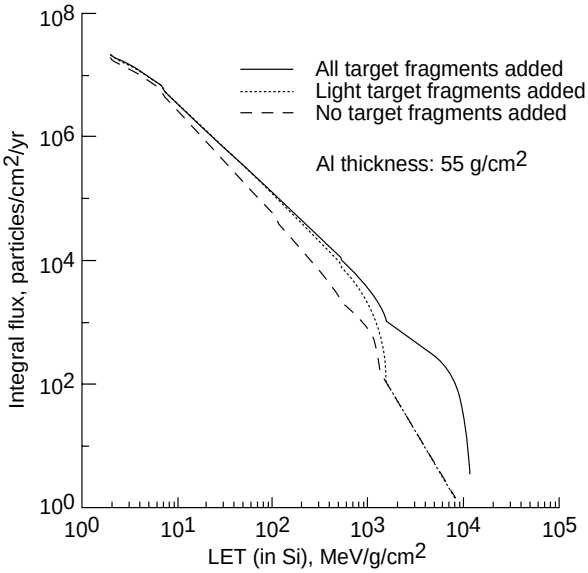

Fig. 4 Calculated integral LET spectra at 55 g/cm^2 depth in aluminum shield exposed to GCR at STS-56 flight conditions. Contributions from all the target fragments added, light ion target fragments, and no target fragments added are shown separately.

The production and accumulation of light ions as GCR propagate through a shield are illustrated in Figure 5 for STS-56 environment. The flux for primary ^{4}He particles with a peak near 1000 MeV/A is seen to decrease with the depth in the shield while the secondaries from target fragmentation accumulate at low energies which correspond to high LET. The isotope ^{3}He is shown to accumulate with low energy fragments. A similar situation applies to deuteron and triton which has less contributions to SEU rates because of lower stopping power than helium.

The modified GCR fluxes due to atomic and nuclear reactions with the Shuttle shield material as described above are then used in equation (15) to predict SEU rate at a given shield depth. Some of the results are shown in Tables II and III for STS-56 (57.1 degree inclination) and STS-51 (28.5 degree) flights, respectively. The contributions from various radiation components are also listed. In general, at thinner shield thicknesses, the rate is dominated by the projectiles and their fragments, but for thick shields light and heavy target fragments dominate. For the lower inclination orbit (STS-51), the ratio of SEU rates from target fragment contribution to the total is generally higher since there is a higher proportion of high energy incident GCR particles which produce target fragments as compared to high inclination orbit. Note that the representation by equivalent aluminum thickness for all the orbiter walls and other structure materials in current and prior [12] analysis is only an approximation as far as nuclear reaction is concerned (see, for instance, reference [27] about the effect from choice of material).

The individual upset rates calculated above for each thickness are then weighted over the orbiter shield distribution shown in Table I to obtain the final SEU rates as listed in Table IV. Also listed are the flight data and previous works [12] for comparison. The observed upset rates on Shuttle flights have been reduced in reference [12] into separate contributions from GCR and SAA (South Atlantic Anomaly) with the GCR rates listed in Table IV. In our present analysis the ratio of SEU rates for two orbits is 3.8:1 versus 2.8:1 from flight data while the prior analysis gives 4.7:1, indicating that the current analysis is more consistent with the flight data when considering the differences in the two incident GCR spectra. Note that a good agreement between flight data and prior analysis [12] in absolute values is fortuitous since the analysis was based on linear relationship between range and energy used in their model and the charge collection length embedded in their model can vary indefinitely with choice of summation steps as discussed in Section III. Furthermore, it was shown in Figure 9(a) of reference [12] in comparing their predicted upset rates with flight data that no consistency between sets of low and high inclination orbits can be reached when they vary their device sensitive volume thickness to width ratio. The listed results in Table IV for their analysis is for their best compromised value of device sensitive volume thickness to width ratio.

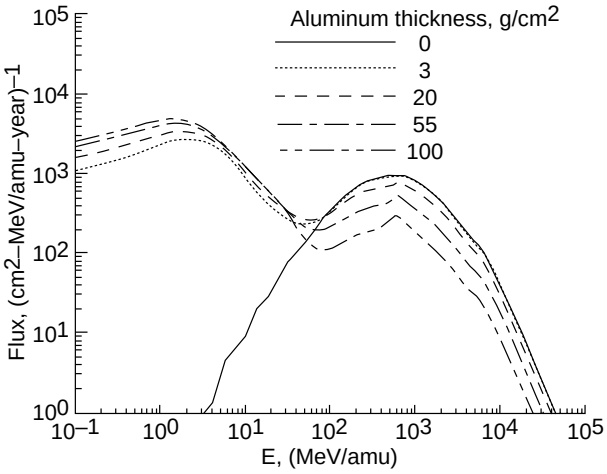

Fig. 5(a) ^{4}He

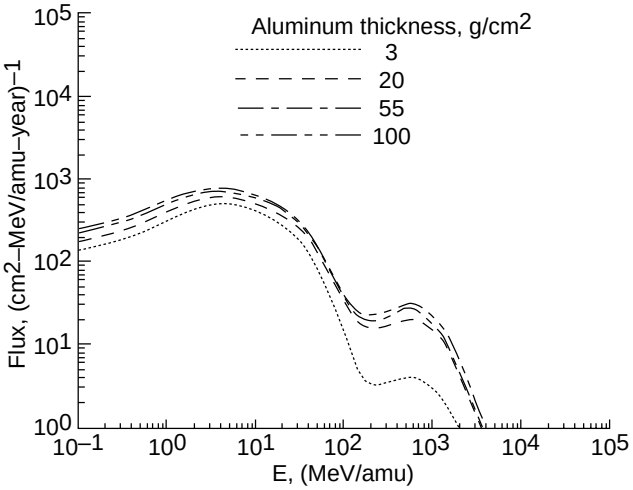

Fig. 5(b) ^{3}He

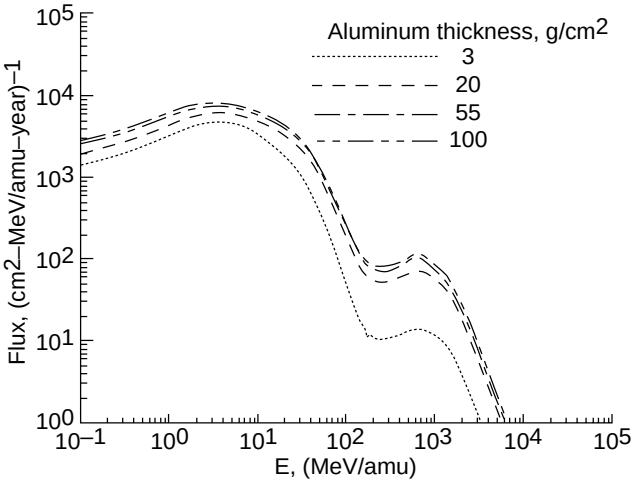

Fig. 5(c) ^{3}H

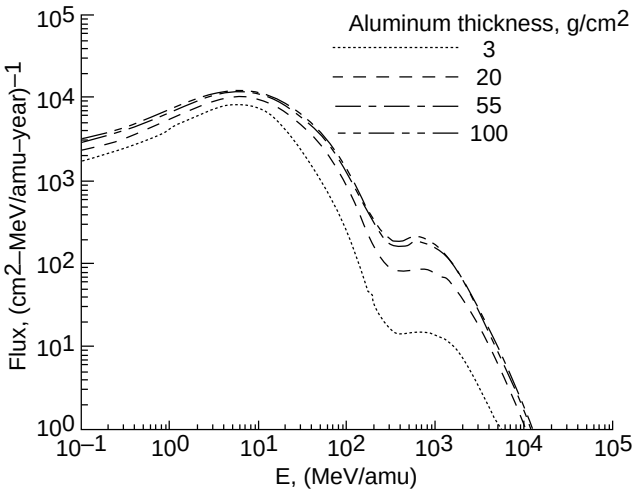

(d) ^{2}H

Fig. 5 Production and accumulation of light ions at GCR propagates through aluminum shield at STS-56 flight conditions.

In current analysis, there are several uncertainties associated with the calculated results. Obviously, the degree of charge recombination and charge collection length are not exactly known. The crude selection of these parameters is permissible when considering other assumptions existing in conventional SEU model, such as rectangular parallelpiped shape for sensitive volume [28]. Errors are also often introduced in reducing measured cross section data into a single curve [20]. Note that the cross-section data shown in Figure 3 do not allow further refinement to the existing curve for the present analysis since the raw data were not available.

Table II. SEU Contribution From Various Radiation Components Behind Several Shield Thicknesses for STS-56 (upsets per day per computer)

Aluminum thickness, g/cm^2	0	3	5	20	55	100
Projectiles and projectile fragments	7.08	7.48	6.95	3.61	.78	.12
Light target fragments (Z=1,2)	0	.70	.73	.91	1.17	1.32
Heavy target fragments (Z>2)	0	.58	.60	.65	.76	.84
Total	7.08	8.76	8.28	5.17	2.71	2.28

Table III. SEU Contribution From Various Radiation Components Behind Several Shield Thicknesses for STS-51 (upsets per day per computer)

Aluminum thickness, g/cm^2	0	3	5	20	55	100
Projectiles and projectile fragments	1.30	1.16	1.08	.62	.17	.04
Light target fragments (Z=1,2)	0	.36	.39	.51	.72	.89
Heavy target fragments (Z>2)	0	.24	.26	.29	.37	.46
Total	1.30	1.76	1.73	1.42	1.26	1.39

Table IV. Comparison of Flight Data and Analyses for SEU Rates (upsets per day per computer)

	Flight Data	Previous Analysis	This work
STS-51	2.13	1.33	1.52
STS-56	6.05	6.26	5.85

VI. CONCLUSIONS

A more consistent set of predictions for SEU rates observed in two Shuttle flights for low and high inclination orbits is obtained in this study than prior analysis which does not contain target fragmentation. The current analysis uses HZETRN which has been compared favorably with flight data obtained by various types of detector responses not limited to microelectronic response. It is clear in the comparison of the HZETRN prediction with the D1 track data that in addition to a correct environmental model one must have an adequate nuclear data base and computational procedures to estimate the particle flux-energy spectra within the shield material. The uniqueness of the Langley transport code development lies in the requirement of laboratory validation with well defined ion beams and target materials [24,25,26]. This is especially important in the low and intermediate LET region where heavy target fragment contributions are modest (LET < 300 $MeV/g/cm^2$). At higher LET, the prediction of etchable tracks must account for limitations of the detector foils since many high LET tracks are lost in post exposure processing. Attention to such details are beginning to close the gap between flight data and prediction. A similar attention to detail has been required to understand the TEPC data as well. We likewise find that evaluation of target fragmentation effects in SEU must be approached by accounting for some of the limitations on the generation and collection of charge within the device. In the case of SEU, we not only treat the distribution of upset sensitivity within the device elements but must allow for the longitudinal and lateral characteristics of the track structure and Auger recombination within the track. Attention to such details will further close the gap between predictions and observations for the shuttle computer SEU data.

VII. ACKNOWLEDGMENTS

We wish to extend our appreciation to Dr. L. W. Connell of Sandia National Laboratories for helpful discussions

VIII. REFERENCES

[1] E. L. Petersen, J. H. Adams, Jr. and E. C. Smith, "Rate predictions for single event effects—a critique," *IEEE Trans. Nucl. Sci.*, Vol. NS-39, pp. 1577–1599, 1992.

[2] G. D. Badhwar and P. M. O'Neill, "An improved model of galactic cosmic rays for space exploration missions," *Nuclear Track and Radiation Measurements*, Vol. 20, pp. 403–410, 1992.

[3] G. D. Badhwar, F. A. Cucinotta, L. A. Braby and A. Konradi, "Shuttle measurements of LET spectra and comparison with radiation transport models," *Radiation Research*, Vol. 139, pp. 344–351, 1994.

[4] J. W. Wilson, S. Y. Chun, F. F. Badavi, L. W. Townsend and S. L. Lamkin, "HZETRN: A heavy ion nuclear transport code for space radiations," NASA TP-3146, December 1991.

[5] J. W. Wilson, L.W. Townsend, W. Schimmerling, G. S. Khandelwal, F. Khan, J. E. Nealy, F. A. Cucinotta, L.C. Simonsen, J. L. Shinn and J. W. Norbury, 'Transport methods and interactions for space radiations," NASA RP-1257, December 1991.

[6] J. L. Shinn, J. W. Wilson, L. W. Townsend, F. A. Cucinotta, S. Y. Chun and F. F. Badavi, "Computationally efficient space radiation transport codes," *Proceedings of the American Nuclear Society Topical Meeting on New Horizons in Radiation Protection and Shielding*, Pasco, WA, April 26-30, 1992, pp. 171–180.

[7] F. A. Cucinotta, L. W. Townsend, J. W. Wilson, J. L. Shinn, G. O. Badhwar, and R. R. Dubey, "Light ion component of the galactic cosmic ray: nuclear interactions and transport theory," *Adv. in Space Res.*, Vol. 17, pp. 77–86, 1995.

[8] G. D. Badhwar, J. U. Patel, F. A. Cucinotta and J. W. Wilson, "Measurements of the secondary particle energy spectra in the space shuttle," *Radiation Measurements*, Vol. 24, pp. 129-138, 1995.

[9] Peter J. McNuty and Cary E. Farrell, "Proton-induced nuclear reactions in silicon," *IEEE Trans. Nucl. Sci.*, Vol. NS-28, pp. 4007–4012, 1981.

[10] T. Bion and J. Bourrieau, "A model for proton-induced SEU," *IEEE Trans. Nucl. Sci.*, Vol. NS-36, pp. 2281–2286, 1989.

[11] J. R. Letaw and E. Normand, "Guide lines for predicting single event upsets in neutron environments," *IEEE Trans. Nucl. Sci.*, Vol. 38, pp. 1500–1506, 1991.

[12] P. M. O'Neill and G. D. Badhwar, "Single event upsets for space shuttle flights of new general purpose computer memory devices," *IEEE Trans. Nucl. Sci.*, Vol. 41, pp. 1755–1764, 1994.

[13] J. H. Adams, Jr., "Cosmic ray effects on microelectronics, part IV," Naval Research Laboratory Memorandum Report 5901, December 31, 1986.

[14] J. W. Wilson, "Analysis of the theory of high-energy ion transport," NASA TND-8381, 1977.

[15] F. A. Cucinotta, "Calculations of cosmic ray helium transport in shielding materials," NASA TP-3354, 1993.

[16] J. L. Shinn, S. John, R. K. Tripathi, J. W. Wilson, L. W. Townsend and J. W. Norbury, "Fully energy dependent HZETRN (A galactic cosmic-ray transport code), NASA TP-3242, 1993.

[17] M. A. Shea and D. F. Smart, Report No. AFCRL-TR-75-0185, Hanscom, AFB, MA, 1975.

[18] J. H. Adams, Jr., J. R. Letaw, and D. F. Smart, "Cosmic ray effects on microelectronics, Part II: The geomagnetic cutoff effects," Naval Research Laboratory Memorandum Report 5099, May 26, 1983.

[19] B. Weigel, W. Heinrich, E. V. Benton and A. Frank, "Measurements of LET spectra and comparison to models," *Adv. Space Res.*, Vol. 12, pp. 349–354, 1992.

[20] L. W. Connell, P. J. McDaniel, A. K. Prinja and F, W. Sexton, "Modeling the heavy ion upset cross section," *IEEE Trans. Nucl. Sci*., Vol. 42, pp. 73–82, 1995.

[21] Michael A. Xapsos, "Applicability of LET to single events in microelectronic structures," *IEEE Trans. Nucl. Sci*., Vol. 39, pp. 1613–1621, 1992.

[22] R. C. Martin, N. M. Ghoniem, Y. Song and Cable, "The size effect of ion charge tracks on single event multiple-bit upset," *IEEE Trans. Nucl. Sci.*, Vol. NS-34, pp. 1305–1309, 1987.

[23] F. A. Cucinotta, R. Katz, J. W. Wilson and R. R. Dubey, "Heavy ion track-structure calculations for radial dose in arbitrary materials," NASA TP-3497, 1995.

[24] J. L. Shinn, J. W. Wilson, F. F. Badavi, I. Csige, A. L. Frank, and E. R. Benton, "HZE beam transport in multilayered materials," *Radiat. Meas.*, Vol. 23, pp. 57–64, 1994.

[25] J. W. Wilson, M. R. Shavers, F. F. Badavi, J. Miller, J. L. Shinn, and R. C. Costen, "Nonperturbative methods in HZE transport," *Radiat. Res.*, Vol. 140, pp. 241–248, 1994.

[26] J. W. Wilson, J. L. Shinn, L. W. Townsend, R. K. Tripathi, F. F. Badavi, and S.Y. Chun, "NUCFRG2: a semiempirical nuclear fragmentation model," *Nucl. Inst. and Methods B*, Vol. 94, pp. 95–102, 1994.

[27] J. L. Shinn, J. E. Nealy, L. W. Townsend, J. W. Wilson, and J. S. Wood, "Galactic cosmic ray radiation levels in spacecraft on interplanetary missions," Invited paper at the World Space Congress, Washington, DC, August 28-September 5, 1992. *Advances in Space Research*, Vol. 14, pp. 863–871, 1994.

[28] James B. Langworthy, "Depletion region geometry analysis applied to single event sensitivity," *IEEE Trans. Nucl. Sci.*, Vol. 36, pp. 2427–2434, 1989.